

**CCUS: 4430776**

## **Modeling CO<sub>2</sub> Injectivity and Mineral Precipitation Dynamics: An Integrated Thermo-Hydro-Chemical Approach**

Muhammad Taha Chhipa<sup>1</sup>, Touka Elsayed<sup>1</sup>, Esuru Rita Okoroafor<sup>1</sup>

1. Harold Vance Department of Petroleum Engineering, Texas A&M University, College Station, TX, USA

Copyright 2026, Carbon Capture, Utilization, and Storage conference (CCUS) DOI 10.15530/ccus-2026-4430776

This paper was prepared for presentation at the Carbon Capture, Utilization, and Storage conference held in The Woodlands, TX, 30 March – 01 April.

The CCUS Technical Program Committee accepted this presentation on the basis of information contained in an abstract submitted by the author(s). The contents of this paper have not been reviewed by CCUS and CCUS does not warrant the accuracy, reliability, or timeliness of any information herein. All information is the responsibility of, and, is subject to corrections by the author(s). Any person or entity that relies on any information obtained from this paper does so at their own risk. The information herein does not necessarily reflect any position of CCUS. Any reproduction, distribution, or storage of any part of this paper by anyone other than the author without the written consent of CCUS is prohibited.

---

### **1. Abstract**

Mineral precipitation from formation brines remains a major operational challenge for maintaining injectivity during CO<sub>2</sub> storage. This study examines how salts and carbonates form and evolve under different temperature, pressure, and salinity conditions, especially when calcite acts as the cementing phase in the reservoir rock. The goal is to understand what controls scaling, how these reactions affect flow performance, and which operating condition adjustments can help minimize injectivity loss.

A set of non-isothermal thermo-hydro-chemical simulations was carried out to capture the coupled effects of multiphase flow, heat transfer, and mineral reactions. The model system consisted of H<sub>2</sub>O, CO<sub>2</sub>, NaCl, CaCl<sub>2</sub>, and CaCO<sub>3</sub> to represent the primary species controlling precipitation and dissolution. Different injection rates, injection temperatures and salinity levels were tested to mimic realistic reservoir conditions. Scenarios also evaluated how varying the degree of calcite cementation affects permeability and near-wellbore response. The injectivity index was the metric used to compare the different scenarios.

The simulations indicate that higher salinity and lower temperatures favor the precipitation of salt and carbonate, leading to pore throat blockage and a decline in injectivity. When calcite is present, an initial phase of mild dissolution may slightly enhance flow before secondary carbonate precipitation begins to seal the same pathways. Increasing the injection temperature within safe operational limits helps delay precipitation and stabilize performance. Lower injection rates and salinity levels further reduce the risk of scaling.

This work bridges geochemical modeling and field operations by identifying practical levers to control mineral precipitation during CO<sub>2</sub> injection. Adjusting injection temperature, moderating flow rates, and pre-conditioning brine all show measurable benefits. The insights help translate complex mineral–fluid

reactions into operational guidelines for designing injection strategies that preserve injectivity and extend well life for CO<sub>2</sub> storage projects.

## 2. Introduction

Geologic carbon sequestration is a critical strategy to mitigate the impact of climate change by reducing carbon emissions from the atmosphere and pave the way towards a carbon-neutral future. For CO<sub>2</sub> storage, there are various geological formations such as deep saline aquifers, depleted oil and gas reservoirs, and coal beds ([IPCC, 2005](#)). Among the above-mentioned, deep saline aquifers exhibit the greatest storage potential, with an estimated storage capacity of 400 to 10,000 gigatonnes ([Ismail, I. et al., 2023](#)). Their widespread distribution, significant pore volumes, and ability to develop various CO<sub>2</sub> trapping mechanisms make them strong candidates for large-scale storage ([Bachu et al, 2015](#)), which has been demonstrated at various globally deployed commercial projects such as Gorgon project - Australia and Sleipner Project - Norway ([Baig, A.R. et al, 2025](#)).

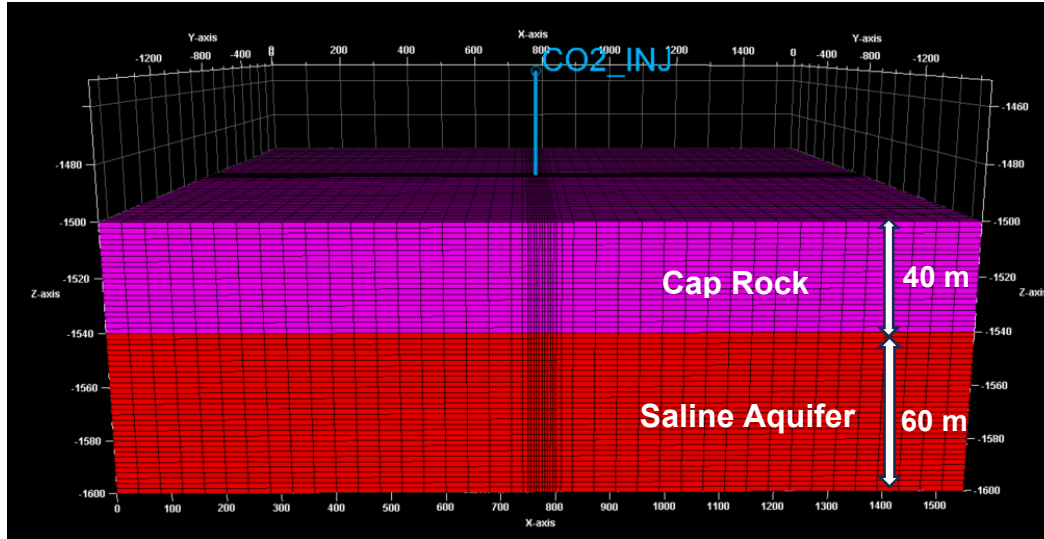
When CO<sub>2</sub> is injected into saline aquifers, it undergoes various geochemical processes, including CO<sub>2</sub> dissolution, brine acidification, and mineral precipitation ([IPCC, 2005](#); [Mitchell, 2010](#)). The initial dissolution can enhance the porosity and permeability of the formation, whereas secondary mineral precipitation can decrease permeability and impede CO<sub>2</sub> injectivity into the formation ([Gaus et al., 2005](#); [Benson et al., 2008](#)). The major challenge is to quantify the effects of fluid-rock interactions on injectivity and long-term storage efficiency in saline aquifers.

Recent studies have focused on examining the kinetics of geochemical reactions during CO<sub>2</sub> sequestration through both laboratory experiments and 3D simulation modeling. [Hussain et al. \(2025\)](#) highlighted that CO<sub>2</sub>-brine reactions with calcite and dolomite may alter injectivity through mineral dissolution and precipitation. [F. Tale et al. \(2025\)](#) have identified permeability enhancement due to CO<sub>2</sub>-saturated brine injection in a calcite-based formation. [Elsayed, T. et al \(2024\)](#) investigated the dissolution of calcite that results in permeability enhancement due to reaction with carbonic acid and the ultimate impact of geochemical reactions in CO<sub>2</sub> Plume Geothermal (CPG) systems using Thermo-Hydro-Chemical-Mechanical (THCM) modeling. [Al Maqbali et al. \(2023\)](#) investigated mineralization phenomena in basaltic formation through sensitivity analyses of reaction kinetics and temperature, and identified a reduction in porosity due to calcite precipitation. [Hussain et al. \(2021\)](#) simulated and demonstrated that CO<sub>2</sub> injectivity and in-situ performance are strongly controlled by CO<sub>2</sub> solubility and reaction kinetics in brine, which govern fluid-rock chemical interactions. All these studies have highlighted the need for coupled Thermo-Hydro-Chemical (THC) modeling of CO<sub>2</sub> dissolution kinetics, which is critical for predicting mineral reactivity and injectivity evolution in subsurface CO<sub>2</sub> applications. In addition to the investigation of reaction kinetics, this study aims to fill a research void by identifying the key operational parameters that can be optimized to mitigate near wellbore precipitation and improve long-term CO<sub>2</sub> storage.

## 3. Theory and/or Methods

### 3.1 Base Model

This study is focused on a hypothetical 3D reservoir simulation model highlighted in Figure 1, featuring a saline aquifer of 60m thickness, capped by a 40m thick layer of impermeable shale. A CO<sub>2</sub> injector well has been placed having a perforation interval ranging from 1590m to 1600m. Table 1 highlights the key parameters of the CO<sub>2</sub> injection system. Multiple simulations were carried out to comprehensively analyze the near wellbore precipitation phenomena. The base case simulation comprised of 1.0 M-Ton/yr injection rate for a period of 6 months, followed by a shutdown period of 3 years. Sensitivity analysis was then performed based on different injection rates, injection temperatures, and formation brine salinities. Solid Saturation, Saturation Diameter, Injection Pressure and Injectivity Index results were compared to gauge the near wellbore permeability reduction.

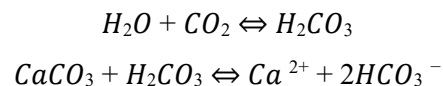
Figure 1: 3D Model representing the CO<sub>2</sub> injection in Saline Aquifer

Symbol	Description	Value	Unit
$k_h$	Horizontal Permeability	250	md
$k_v/k_h$	Permeability Anisotropy	0.3	md
$k$	Shale Permeability	0.001	md
$\Phi$	Shale Porosity	0.2	-
$\Phi$	Reservoir Porosity	0.2	-
$H$	Reservoir Thickness	60	m
$P_r$	Reservoir Pressure	158	bar
$T_r$	Reservoir Temperature	65	°C
-	Brine Salinity	70,000	ppm
$D$	Top of Depth	1500	m

Table 1. Nomenclature and Parameters of the CO<sub>2</sub> injection system

### 3.2 Chemical Interactions

This study was based on a five-component model for CO<sub>2</sub> injection system, consisting of H<sub>2</sub>O, CO<sub>2</sub>, NaCl, CaCl<sub>2</sub>, and CaCO<sub>3</sub>. Following chemical reactions were considered for the modeling:



### 3.3 Injectivity Index

Analogous to the productivity index, the injectivity index quantifies the efficiency of the reservoir in accepting injected fluids and is defined as the ratio of the injection rate to the differential between injection and reservoir pressure. A higher injectivity index exhibits lesser near wellbore permeability impairment,

which is the metric used in this study to compare different injection scenarios. Equation 1 has been used to calculate the injectivity index values for the base-case and sensitivity-analysis simulations.

$$II = \frac{q}{p_{inj} - p_r} \dots\dots\dots (1)$$

where,

II = injectivity index (m<sup>3</sup>/day/bar)

q = injection rate (m<sup>3</sup>/day)

P<sub>inj</sub> = injection pressure (bar)

P<sub>r</sub> = reservoir pressure (bar)

#### 4. Results

##### 4.1 Base Case

The 3D plot in Figure 2 displays the effect of CO<sub>2</sub> injection on solid saturation at an injection rate of 1.0 M-Ton/yr, 35 °C injection temperature, and 70,000 ppm brine salinity. The plot exhibits approximately 2.3% solid saturation with 50 m saturation diameter. Injectivity Index was estimated to be 101,653 m<sup>3</sup>/day/bar against 172 bar injection pressure.

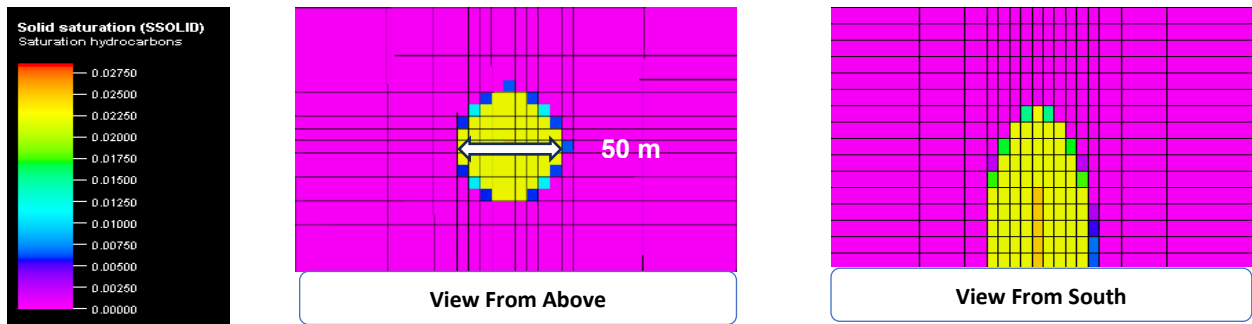


Figure 2. 3D Solid Saturation plot at 1.0 M-Ton/yr injection rate

##### 4.2 Sensitivity Analysis

Multiple simulations were carried out to perform the following sensitivity analysis:

- Injection rate: 0.25 M-Ton/ yr and 0.5 M-Ton/yr
- Injection temperature: 45 °C and 55 °C
- Brine Salinity: 50,000 ppm and 30,000 ppm

Table 2 highlights the simulation results of the base case and sensitivity analysis based on the above-mentioned scenarios:

Case	Injection Scenario	Inj. Rate (M-Ton/yr)	Inj. Temp (°C)	Brine Salinity (ppm)	Solid Saturation (%)	Saturation Diameter (m)	Inj. Pressure (bar)	Injectivity Index (m <sup>3</sup> /day/bar)
1	Base Case	1.0	35	70,000	2.3	50	172	101,653
2	Injection Rate	0.25	35	70,000	2.3	24	160	116,537
3		0.50	35	70,000	2.3	34	164	169,038
4	Injection Temperature	1.0	45	70,000	1.9	50	170	115,229
5		1.0	55	70,000	1.6	50	169	125,704
6	Brine Salinity	1.0	35	50,000	1.5	45	171	106,365
7		1.0	35	30,000	1.2	45	170	115,229

Table 2. Simulation results based on multiple CO<sub>2</sub> injection scenarios

## 5. Discussion

### 5.1 Case 2 and 3:

Simulation results indicate that the saturation diameter reduced with a reduction in the CO<sub>2</sub> injection rate, whereas the solid saturation remained the same. Consequently, injectivity index improved due to reduced injection pressure, indicating less near wellbore permeability reduction due to small precipitation envelope. It exhibits that CO<sub>2</sub> injection system at high injection rate encounter early pressure buildup which impedes further CO<sub>2</sub> injectivity in the formation.

### 5.2 Case 4 and 5:

Simulation results indicate that solid saturation reduced with the increasing CO<sub>2</sub> injection temperature, whereas the saturation diameter remained the same. Consequently, injectivity index improved due to reduced injection pressure, indicating less near wellbore permeability impairment due to reduced mineral precipitation. These results supplement the concept that CO<sub>2</sub> solubility decreases at high temperature which reduces brine acidification and ultimately reduces secondary mineral precipitation.

### 5.3 Case 6 and 7:

Simulation results indicate that both solid saturation and saturation diameter reduced with the decreasing formation brine salinity. Consequently, injectivity index improved due to reduced injection pressure, indicating less near wellbore permeability impairment due to both reduced mineral precipitation and precipitation envelope. It exhibits that brine with low salinity contains less dissolved ions which reduces solid precipitation. CO<sub>2</sub> solubility also increases with decreasing salinity which decreases pressure build-up near wellbore and ultimately improves injectivity.

## 6. Conclusions

This study has examined the coupled effects of multiphase flow, heat transfer, and geochemical reactions to evaluate the evolution of CO<sub>2</sub> injectivity in saline aquifers. The results demonstrate that the near-wellbore mineral precipitation can impede the long-term CO<sub>2</sub> injectivity in subsurface formations due to permeability impairment.

The findings in this study highlight that the optimization of injection rate, injection temperature, and formation brine salinity can aid in reducing the near wellbore mineral precipitation. Lower injection rate, higher injection temperature, and lower salinity can mitigate the near wellbore permeability impairment and ultimately improve the injectivity index.

Overall, this research has incorporated comprehensive THC modeling, which fills a critical research gap by identifying the key operational parameters that can be optimized and aid in improving the efficiency of the CO<sub>2</sub> injection systems.

## 7. References

IPCC (2005). Intergovernmental Panel on Climate Change, *Special Report on Carbon Dioxide Capture and Storage*, Chapter 5: Underground Geological Storage. <https://www.ipcc.ch/report/carbon-dioxide-capture-and-storage/>

Ismail, I.; Gaganis, V. (2023). Carbon Capture, Utilization, and Storage in Saline Aquifers: Subsurface Policies, Development Plans, Well Control Strategies and Optimization Approaches—A Review. *Clean Technol.* 2023, 5, 609–637. <https://doi.org/10.3390/cleantechnol5020031>

Bachu, S., Bonijoly, D., Bradshaw, J. et al (2015). CO<sub>2</sub> storage capacity estimation: Methodology and gaps. *International Journal of Greenhouse Gas Control*, 40, 345–360. <https://doi.org/10.1016/j.ijggc.2015.05.031>

Baig, A.R.; Fentaw, J.; Hajiyev, E.; Watson, M et al (2025). Comprehensive Insights into Carbon Capture and Storage: Geomechanical and Geochemical Aspects, Modeling, Risk Assessment, Monitoring, and Cost Analysis in Geological Storage. *Sustainability* 2025, 17, 8619. <https://doi.org/10.3390/su17198619>

Mitchell, A. C., Phillips, A. J., Hiebert, R. et al (2010). Biofilm enhanced geologic sequestration of supercritical CO<sub>2</sub>. *International Journal of Greenhouse Gas Control*, 4(3), 400–408. <https://doi.org/10.1016/j.ijggc.2009.05.002>

Gaus, I., Azaroual, M., & Czernichowski-Lauriol, I. (2005). Reactive transport modelling of the impact of CO<sub>2</sub> injection on the clayey cap rock at Sleipner (North Sea). *Chemical Geology*, 217(3–4), 319–337. <https://doi.org/10.1016/j.chemgeo.2004.12.016>

Benson, S. M., & Cole, D. R. (2008). CO<sub>2</sub> sequestration in deep sedimentary formations. *Elements*, 4(5), 325–331. <https://doi.org/10.2113/gselements.4.5.325>

S. Hussain; B. R. B. Fernandes; M. Delshad; K. Sepehrnoori (2025). History Matching Naturally Fractured Carbonate Gas Condensate Reservoir Performance for CO<sub>2</sub> Storage. <https://doi.org/10.2118/228065-MS>

Fatemeh Tale, Abdulrahman Abdulwarith, Feiyan Chen et al (2025). Dynamics of Permeability Changes in CO<sub>2</sub> Saturated Brine Injection: An Integrated Modeling Approach. <https://doi.org/10.15530/ccus-2025-4184874>

Elsayed, T., Okoroafor, E. R. (2024). Integrated Thermo-Hydro-Chemo-Mechanical (THCM) Analysis for Evaluating CO<sub>2</sub> Plume Geothermal System Potential. <https://doi.org/10.2118/220927-MS>

Qais Al Maqbali; Sadam Hussain; Gene Mask; Wu Xingru (2023). Numerical Simulation of In-Situ CO<sub>2</sub> Mineralization in Mafic Basaltic Formations in Southwest Oklahoma. <https://doi.org/10.2118/213084-MS>

Sadam Hussain; Xingru Wu; Ben Shiau (2021). Numerical Mechanistic Study of In-Situ CO<sub>2</sub> EOR – Kinetics and Recovery Performance Analysis. <https://doi.org/10.2118/206292-MS>